

Crystallization kinetics of highly filled glass fibre/polyamide 6 composites

G. Hinrichsen* and F. Lux

Technical University of Berlin, Institute of Nonmetallic Materials, Polymer Physics, Englische Str. 20, D-1000 Berlin 12

Summary

The present paper deals with the isothermal and non-isothermal crystallization of pure polyamide 6 (PA 6) and PA 6/glass fibre composite with a high fibre content of 81 % by weight. The so-called Avrami exponent n of pure PA 6 seems to be nearly independent of crystallization temperature fluctuating around 3.0 whereas for the composite this quantity increases strongly with crystallization temperature from 1.2 to about 6.

Introduction

The crystallization kinetics of numerous semicrystalline polymers have been investigated since the beginning of industrial production of these materials. Investigations of this kind on polyamide have been carried out by various authors (1)–(6) while analogous investigations on highly filled glass fibre/polyamide composites are very scarce in the literature (7).

In order to investigate the crystallization kinetics various methods have been applied, e.g. dilatometric, densitometric, light-microscopical, X-ray wide angle, and calorimetric methods. The last one, usually realized by DSC or DTA measurements, has been proven as a practicable and successful way. The crystallization kinetics can be observed either by isothermal or by non-isothermal mode both of which can be carried out using DSC technique.

Due to the low portion of crystallizable polymeric material within the composite it has to be expected that the crystallization behaviour differs from that of pure polyamide. The influence of the fibre surface as a nucleating agent as well as the interaction forces between glass fibres and macromolecules have to be taken into consideration with regard to the crystallization kinetics.

Experimental

The polyamide 6 sample used in this study was a commercial grade Durethan B 31 F produced by BAYER AG, Leverkusen.

The glass fibre/polyamide 6 composite was produced by a pultrusion equipment described elsewhere (8). The glass fibre content of the ribbon like specimens was kept constant at 81 % by weight. The high content of glass fibres gives rise to an average thickness of the polyamide matrix of only approximately 2 μm . The exact value depends on the glass fibre diameter. The glass fibre content of the composite was determined gravimetrically after reducing to ashes at 600°C.

Light microscopical investigations were carried out in a Leitz polarizing microscope and scanning electron micrographs were recorded using a Cambridge Stereoscan 180.

*To whom offprint requests should be sent

A Perkin Elmer DSC-1B was used for the determination of crystallization kinetics, melting and crystallization temperatures, and heats of fusion and crystallization. The sample crystallization was performed either at constant temperature in the range from 474 - 484 K or at constant cooling rates after being held in the molten state at 523 K for 30 min. Measurements have been carried out by purging the DSC cell with gaseous nitrogen. The crystallization exotherms were recorded at selected cooling rates: 1, 2, 4, 8, 16, 32 K/min.

Prior to DSC investigations the samples have been dried under vacuum at 373 K for 72 hours and subsequently stored in an exsiccator till measurement.

In the case of pure PA 6 samples the weight of the DSC specimens amounted to about 10 mg and in the case of composites to about 25 mg (i.e. at about 5 mg PA 6). Calibration of temperature and heat of fusion (crystallization) was carried out for each heating (cooling) rate using indium and tin as standards.

Isothermal and non-isothermal crystallization

The isothermal crystallization of crystallizable polymers is described by the well-known Avrami equation (9)

$$1 - X(t) = \exp(-k \cdot t^n) \quad (1)$$

with

$X(t)$ mass percentage of crystallized material at time t
(crystalline fraction)

k crystallization constant

n Avrami constant depending on nucleation type, geometrical factors, and crystal growth mechanism.

Normally, the double logarithm of the reciprocal amorphous fraction $\log(-\ln(1 - X(t)))$ at constant temperature is plotted as a function of $\log t$ (Avrami plot). If equation (1) is valid, the curve corresponding to each temperature should be a straight line and the constants k and n can be obtained.

Only a few theories have been developed in order to study the kinetics of non-isothermal crystallization (10) - (13). In this paper the former theory of Ozawa (11) will be applied for the analysis of DSC cooling curves. An equation similar to (1) has been derived

$$1 - X(T) = \exp(-k^*(T)/a^n) \quad (2)$$

with

$k^*(T)$ so-called cooling crystallization function

a (constant) cooling rate.

The representation of $\log(-\ln(1 - X(T)))$ as a function of $\log a$ at constant temperature allows the determination of values of the crystallization function $k^*(T)$ and of the Avrami constant n . Restrictions of eq.(2) are given by the fact that two factors were neglected by Ozawa in the derivation of the equation, namely slow secondary crystallization and changes of crystal thickness (fold length) in dependence on temperature during dynamic crystallization.

The quantities $X(t)$ and $X(T)$ resp. were determined by stepwise integration of the DSC curves, either in the isothermal or in the cooling mode. $X(t)$ and $X(T)$ resp. were set to unity for the complete DSC crystallization peak.

Results and discussion

Figs. 1 and 2 show the results of the investigations of the isothermal crystallization of pure PA 6 and PA 6/glass fibre composites. As clearly

demonstrated by the Avrami plot of the results the crystallization process cannot be described as a unique one. The lines in Figs. 1 and 2 show continuously changing curvatures which are approached by two straight lines in a more or less good approximation. From the slope of the straight lines the Avrami exponents n were calculated which are represented in Fig. 7 and discussed later on.

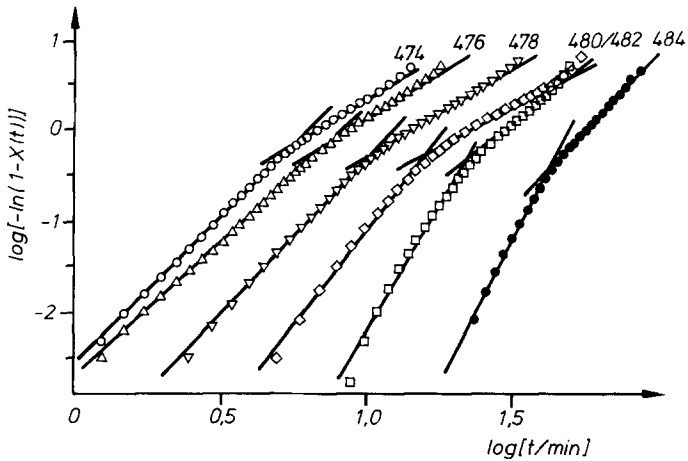


Fig. 1: Avrami plot of isothermal crystallization of pure PA 6 according to eq. (1). Crystallization temperatures as indicated.

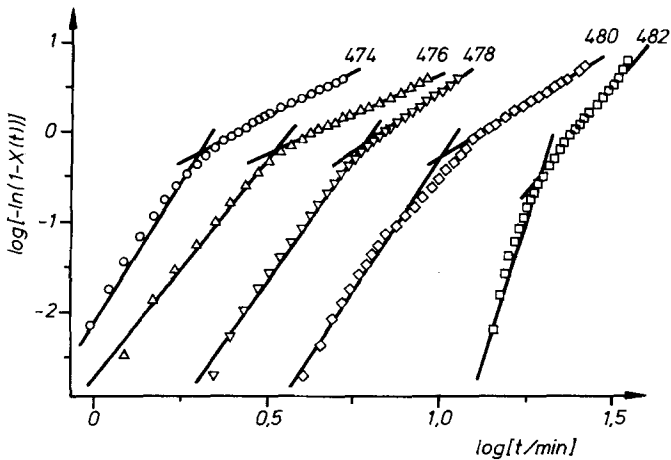


Fig. 2: Avrami plot of isothermal crystallization of PA 6/glass fibre composites according to eq. (1). Crystallization temperatures as indicated.

The differences in the crystallization behaviour between pure PA 6 and PA 6/glass fibre composite can also be demonstrated by measuring the half-time for crystallization (s. Fig. 3). The crystallization of the PA 6

component within the composite runs significantly faster than the respective bulk polymer.

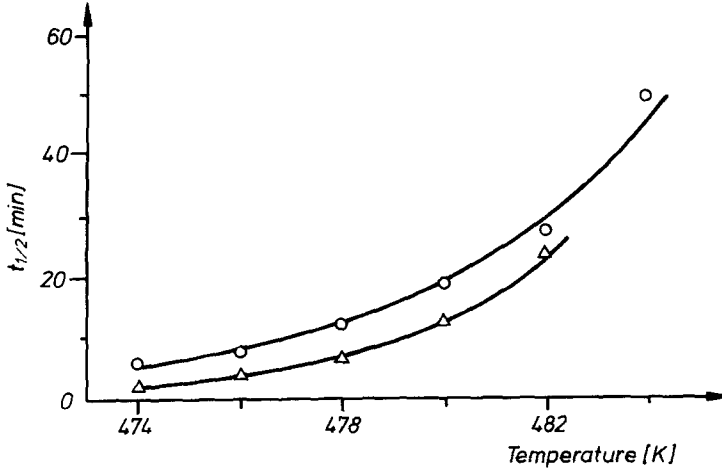


Fig. 3: Half-time for crystallization of pure PA 6 and PA 6/glass fibre composite resp. in dependence on crystallization temperature.
 \circ Bulk PA, \triangle PA 6/glass fibre composite.

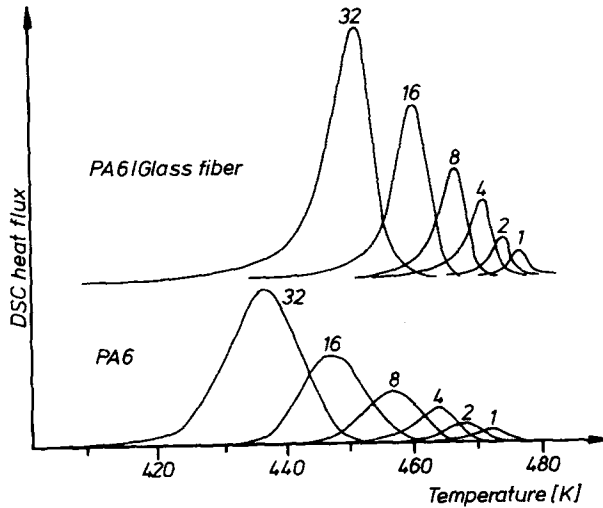


Fig. 4: Influence of cooling rate on non-isothermal crystallization of pure PA 6 (lower part) and PA 6/glass fibre composite (upper part). The DSC curves are standardized for 1 mg PA 6. Cooling rates as indicated.

The DSC diagrams of the non-isothermal crystallization of both bulk PA 6 and PA 6/glass fibre composite in dependence on cooling rate are arranged in

Fig. 4, from which differences in the maximum peak temperature and the half-width of the crystallization exotherms can easily be observed. Fig. 5 shows the maximum peak temperature as a function of the cooling rate; the difference between the temperature of crystallization maximum of pure PA 6 and PA 6/glass fibre composite grows on with increasing cooling rate and reaches at about 15 K for the heating rate 32 K/min. As an example, in Fig. 6 the noncrystalline fraction is plotted in dependence on temperature during crystallization process with a cooling rate of 2 K/min. This figure confirms the shift of the crystallization interval to lower temperature and the broadening of this interval for pure PA 6 in comparison with PA 6/glass fibre composite.

According to eq. (2) the Avrami constant n can also be obtained from the non-isothermal crystallization curves by plotting the quantity $\log(-\ln(1 - X(T)))$ as a function of $\log a$. Due to the fact that only a few selected cooling rates could be applied (fixed by the used Perkin Elmer DSC-1B apparatus) the straight lines according to eq. (2) are determined by two or at maximum three measured values. This effect leads to the result that the slope of the straight lines which represents the Avrami constant n cannot be calculated with high precision. Therefore, high experimental scatter of this quantity has to be expected.

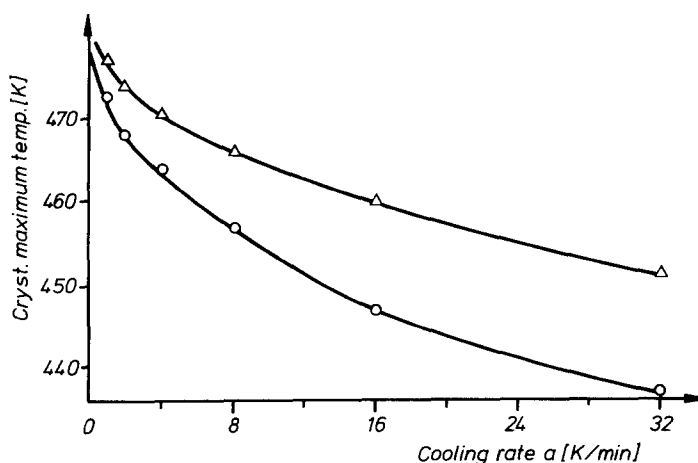


Fig. 5: Temperature of crystallization maximum in dependence on cooling rate.
 \circ Bulk PA 6, \triangle PA 6/ glass fibre composite.

Fig. 7 shows the combined results of the investigations of the isothermal as well as of the non-isothermal crystallization kinetics within the temperature interval 440 - 484 K. The Avrami exponent n of pure PA 6 fluctuate around $n = 3.0$ with increasing tendency at higher temperatures. At the highest (isothermal) crystallization temperatures (482 and 484 K) values of $n \approx 4-5$ are observed. It has to be mentioned that only the slope of the straight lines which represents the beginning of the crystallization (s. Fig. 1) was used for the calculation of the values of n in Fig. 7. The slope of the straight lines representing the second part of the crystallization process leads to lower values of n in the range of 1.7 - 3.0.

In contrast to the restricted dependence of the Avrami exponent for bulk PA 6 this quantity varies in a much wider range for the PA 6/glass fibre

composite. Starting with values $n \approx 1.2 - 1.5$ at $T = 440$ K the Avrami constant reaches $n \approx 3$ at about $T = 470$ K and grows on to $n \approx 6$ at $T = 480$ and 482 K (isothermal crystallization mode). Avrami exponents $n \approx 5 - 6$ are reported very rarely in the literature and may point to a complicated structural growth (14). On the other hand, very low values of $n = 1 - 2$, as observed during the non-isothermal crystallization by cooling from the melt may indicate the formation of a more fibrillar morphology.

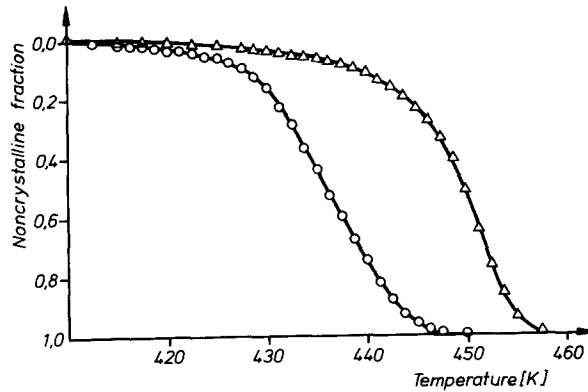


Fig. 6: Non-isothermal crystallization of pure PA 6 and PA 6/glass fibre composite. Noncrystalline fraction in dependence on temperature. Cooling rate: 2 K/min.: \circ Bulk PA 6, \triangle PA 6/glass fibre composite.

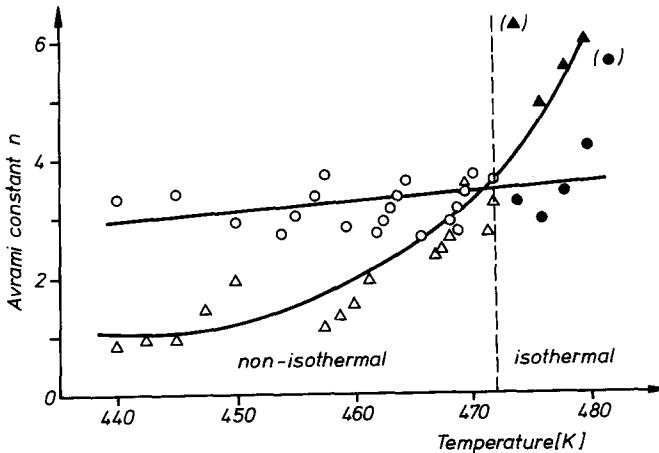


Fig. 7: Avrami exponent n in dependence on crystallization temperature.
Bulk PA 6: \circ non-isothermal crystallization, \bullet isothermal crystallization.
PA 6/glass fibre composite: \triangle non-isothermal crystallization, \blacktriangle isothermal crystallization.

In order to prove this suggestion light and electron scanning microscopical investigations of polished cuts of non-isothermally crystallized PA 6/glass fibre composites were carried out. Fibrils with an average diameter of about 2 μm are running from glass fibres to the neighbouring ones. It has to be mentioned, however, that at present an influence of the polishing procedure on the observed morphology can not be completely excluded. Careful investigations on this matter are planned for the near future.

The various crystallized specimens were heated up in the DSC and the heats of fusion were recorded (s. Tab. 1). The heat of fusion of both types of specimens decreases with increasing cooling rate indicating the reduced crystallization at higher cooling rates as expected. It is noticeable that the decrease of the heat of fusion of the PA 6/glass fibre composite with increasing cooling rate is much lower for the composite material than for the bulk PA 6.

Table 1: Heat of fusion of pure PA 6 and PA 6/glass fibre composites crystallized by cooling from the melt with different cooling rates. Heating rate: 10 K/min.

Cooling rate [K/min]	2	4	8	16	32
Bulk PA 6 [J/g]	86.5	77.5	75.5	70.5	62.0
Composite [J/g]	73.0	72.0	70.5	67.5	66.0

Conclusion

The investigations of crystallization kinetics on pure and glass fibre reinforced polyamides reveal big differences as shown in this paper. With pure PA 6 the Avrami constant was found in the range of about $n = 3$ depending only slightly on crystallization mode and temperature. This conclusion is in accordance with results reported in the literature (1, 3, 5, 7).

With PA 6/glass fibre composite a strong dependence of the Avrami exponent in the interval from $n = 1.2$ until $n = 6$ on the crystallization temperature was observed. The result confirms exactly the data of Chabert et al. (7) who discovered a strong increase of the Avrami exponent with crystallization temperature for the system PA 6,6/glass fibre ($n = 0.5 - 5.0$). The percentage of glass fibre in this composite had amounted to 70% by weight.

For the present, the strong dependence of the Avrami constant on the crystallization temperature can not be considered as fully understood. According to Wunderlich (14) "additional information on nucleation, morphology, and possibly even mechanism is necessary to fully interpret the exponent n ". This means that our investigations of crystallization kinetics and morphology have to be continued. Furthermore, the fact has to be taken into account that due to the presence of the glass fibres the heat capacity and the thermal conductivity will be influenced, a problem which has been neglected up to now. Finally, it has to be considered that as a consequence of the small distances of the glass fibres (1 - 2 μm) the growing morphological entities (fibrils, spherulites, any other morphological formations) are prohibited to extend in an undisturbed manner but early meet with the surrounding boundaries.

Acknowledgement

The help of Dr. Augustin and Dr. H.-J. Traenckner, BAYER AG, Leverkusen, who prepared the PA 6/glass fibre composites, is gratefully acknowledged. The

investigations were supported by the Bundesminister für Forschung und Technologie (BMFT) under Grant No. 03 M 1002 A 3.

References

1. J.H. Magill, *Polymer* 3, 252 (1962)
2. J.V. McLaren, *Polymer* 4, 175 (1963)
3. E. Turska, G. Gogolewski, *Polymer* 12, 616 (1971);
12, 629 (1971)
4. W. Kozłowski, *J. Polym. Sci. C* 38, 47 (1972)
5. A. Savolainen, *J. Polym. Sci. Polym. Symp.* 42, 885 (1973)
6. B. Monasse, N. Billon, J.M. Haudin, *Calorim. Anal. Therm.* 16,
114 (1985)
7. B. Chabert, J. Chauchard, J. Cinquin, *Macromol. Chem. Macromol.*
Symp. 9, 99 (1987)
8. G. Augustin, G. Hinrichsen, and H.-J. Traenckner, *Kunststoffe*,
to be prepared
9. M.J. Avrami, *J. Chem. Phys.* 7, 1103 (1939); 8, 212 (1940)
10. A. Ziabicki, *Appl. Polym. Symp.* 6, 1 (1967)
11. T. Ozawa, *Polymer* 12, 150 (1970)
12. K. Harnisch and H. Muschik, *Coll. Polym. Sci.* 261, 908 (1983)
13. T. Ozawa, *Thermochim. Acta* 135, 85 (1988)
14. B. Wunderlich, *Macromolecular Physics Vol. 2*, Academic Press,
New York 1975, p. 147

Accepted April 18, 1990

C